A&A 395, L5–L8 (2002)
DOI: 10.1051/0004-6361:20021419

Astronomy & Astrophysics

Letter to the Editor

The kinetic temperature of Barnard 68⋆

S. Hotzel, J. Harju, and M. Juvela

Observatory, PO Box 14, 00014 University of Helsinki, Finland

Received 12 September 2002 / Accepted 26 September 2002

Abstract. We have observed the nearby isolated globule Barnard 68 (B68) in the $(J, K) = (1, 1)$ and $(2, 2)$ inversion lines of ammonia. The gas kinetic temperature derived from these is $T = 10 \pm 1.2$ K. The observed line-widths are almost thermal: $\Delta V = 0.181 \pm 0.003$ km s^{-1} ($\Delta V_{\rm therm} = 0.164 \pm 0.010$ km s^{-1}), supporting the earlier hypothesis that B68 is in hydrostatic equilibrium. The kinetic temperature is an input parameter to the physical cloud model put forward recently, and we discuss the impact of the new value in this context.

Key words. ISM: individual objects: Barnard 68 – ISM: abundances – ISM: molecules

1. Introduction

Discovered by Barnard (1919), the isolated, starless globule Barnard 68 (B68) received increased attention recently, after Alves et al. (2001) presented a high resolution extinction map and a cloud model, suggesting that B68 has the physical structure of a so-called Bonnor-Ebert sphere (BES, i.e. a pressure bound, isothermal sphere in hydrostatic equilibrium). With its column density and thus number density profiles revealed, B68 became an ideal object to study molecular depletion in dark core interiors (Bergin et al. 2002; Hotzel et al. 2002, hereafter Paper I), molecular abundances for a number of species (Di Francesco et al. 2002) and the gas-to-dust ratio (Paper I).

The BES cloud model as based on the measurements of Alves et al. (2001) fixes the normalised profiles of the density ($n/n_{\rm c}$) and the column density ($N/N_{\rm c}$) as functions of the normalised radius (r/R), while for the absolute values of the central density $n_{\rm c}$, the central column density $N_{\rm c}$ and the radius R additional measurements are necessary. The knowledge on any two of the parameters $n_{\rm c}$, $N_{\rm c}$, D (distance) and T (kinetic temperature) settles the others (Paper I). The column density is linked to the extinction profile also via the *gas-to-dust ratio* (we use this term as short form for the more precise *hydrogen column density per unit reddening by dust*). Hence, if the BES model holds, one can determine the gas-to-dust ratio if D and T are known, or one can determine the distance to the cloud by measuring T and applying a "standard" gas-to-dust ratio. In any case, the kinetic temperature remains the key parameter to measure. A reliable temperature measurement in cold, dense cores is possible using the 1.3 cm lines of ammonia (Walmsley & Ungerechts 1983; Danby et al. 1988). However, previous ammonia measurements ($T = 16$ K, Bourke et al. 1995) are in contradiction to other temperature derivations (Avery et al. 1987, Paper I).

Here we present new ammonia measurements, carried out with the Effelsberg 100-m telescope. Apart from the temperature derivation and an assessment of the inherent uncertainties, we compare the line-width to the width expected from purely thermal motion, which is a crucial test of the assumption that B68 is in hydrostatic equilibrium. We calculate the distance, gas-to-dust ratio and fractional ammonia abundance that follow from the BES model and the new temperature value.

2. Observations and data calibration

The $(J, K) = (1, 1)$ and $(2, 2)$ inversion lines of NH_3 were observed simultaneously on May, 6th, 2002 with the Effelsberg 100-m telecope (40″ beam at 23.7 GHz). B68 was between 12.2° and 15.8° (max) elevation. We used the new 1.3 cm HEMT (High Electron Mobility Transistor) receiver in the frequency switching mode. The system temperature including the atmosphere was 63–74 K. The spectrometer was a 8192 channel autocorrelator split into four quarters, two for each polarization channel, centred on the frequencies of the $(J, K) = (1, 1)$ and $(2, 2)$ transitions, $\nu_0(1, 1) = 23.694495487$ GHz and $\nu_0(2, 2) = 23.722633335$ GHz respectively (line parameters from Kukolich 1967). The velocity resolution was 0.062 km s^{-1}. Pointing was checked on NGC 7027 and NRAO 530 and was found to be better than 6″.

The data were calibrated using NGC 7027, for which we assumed an observed flux density of $F_\nu(23.71\ {\rm GHz}) = 4.99$ Jy (Ott et al. 1994). This value takes into account the spatial extension of the source (true flux is 1.5% higher) and the epoch of the observation (annual flux decrease is 0.5%). We multiplied the spectra with a gain-elevation correction factor based on the measurements of Altenhoff (1983, private communication),

Send offprint requests to: S. Hotzel,
e-mail: hotzel@astro.helsinki.fi

⋆ Based on observations with the 100-m telescope of the MPIfR (Max-Planck-Institut für Radioastronomie) at Effelsberg.

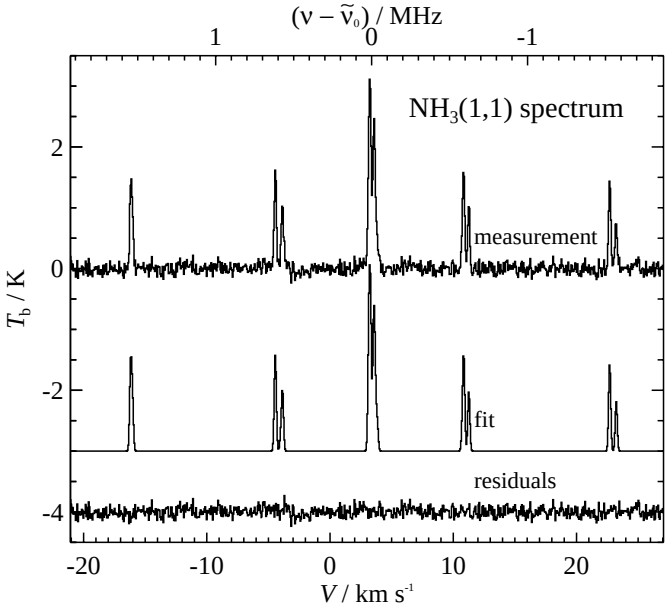

Fig. 1. B68 as observed in the $(J, K) = (1, 1)$ inversion transition of NH_3. The position observed is $\alpha(2000) = 17^h22^m46\overset{s}{.}0$, $\delta = -23°49'48''$. The y-axis gives the brightness temperature, T_b. The upper x-axis gives the frequency offset from the central frequency of the transition, $\nu_0(1, 1)$, corrected for the relative velocity of the cloud. The velocity axis corresponds to $\nu_0(1, 1)$ and its zero point refers to $\nu_0(1, 1)$ in the $V_{lsr} = 0$ frame. Top: calibrated spectrum after a total of 134 min effective integration time. Middle (shifted by −3 K for visibility): χ^2-fit assuming LTE among the 18 hyperfine components and taking the velocity resolution of the spectrometer into acccount. Down (shifted by −4 K): residual spectrum after subtracting the fit.

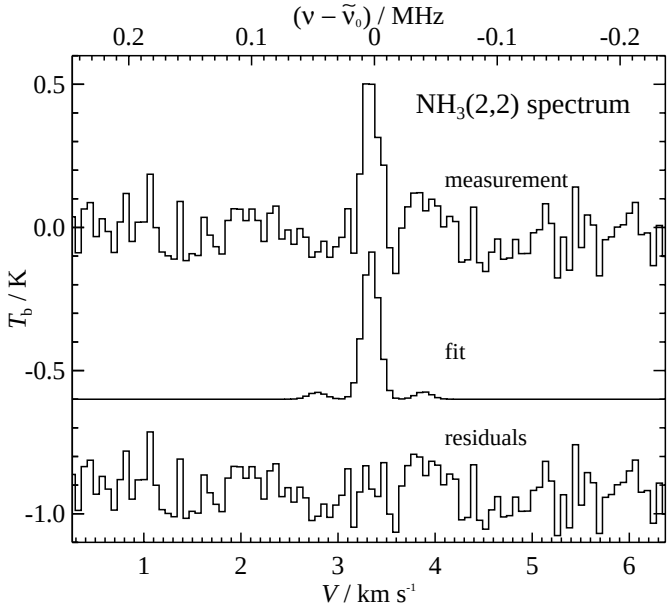

Fig. 2. B68 as observed in the $(J, K) = (2, 2)$ inversion transition of NH_3. For observed position, integration time and description of plotting axes see Fig. 1. Top: calibrated spectrum. The noise is still too high (and the temperature too low) to see the weaker hyperfine components. Middle (shifted by −0.6 K for visibility): χ^2-fit, the fitted parameters are V_0 and $\tau_0(2, 2)$. The parameters T_{ex} and ΔV are kept fixed using the values derived in the $(1, 1)$ fit. Down (shifted by −0.9 K): residual spectrum after subtracting the fit.

which are consistent with more recent observations at intermediate elevations provided by the telescope team. The values for the receiver sensitivity and main beam efficiency were 0.93 K/Jy and 58% respectively. The uncertainties of the calibration are (1) the uncertainty of the absolute flux density of the calibration source, (2) the statistical error of our calibration measurements (changes in atmospheric conditions, telescope gain, etc.) and (3) the remaining uncertainty of the gain-elevation dependency at very low elevations. They add up to 20%. Summing, folding and baseline-fitting were done using CLASS. Unfortunately, one of the polarization channels showed differences between the on- and off-frequency spectra (possibly due to a sensitivity gradient of the receiver) and also a variation of the spectra with time. As we could not reliably correct for these artifacts, we decided to discard that channel in the following analysis. The calibrated spectra, obtained with a total effective integration time of 134 min, are shown in Figs. 1 and 2. The beam filling factors assumed are $\eta(1, 1) = \eta(2, 2) = 1$.

3. Results

The general concept of deriving cloud parameters from the hyperfine spectra is presented by Ho et al. (1979). NH_3 fundamentals can be found e.g. in the papers of Kukolich (1967), Poynter & Kakar (1975) and in the review by Ho & Townes (1983). In order to derive reliable values for the intrinsic line-width we have convolved the model spectrum with the filter frequency response function (approximated by a Gaussian with full width at half maximum (*FWHM*) of 1 channel-width) when finding the best model spectrum in a χ^2-fit to the data. Each channel was weighted with the inverse square of the rms (root-mean-square) noise of the spectrum determined outside the lines. For the (1, 1) spectrum, the four unknown variables excitation temperature T_{ex}, total opacity $\tau_0(1, 1)$, line-of-sight velocity V_0 and line-width ΔV can be determined from the spectrum. The weaker hyperfine lines of the (2, 2) spectrum allow only for the fitting of two unknowns, namely $\tau_0(2, 2)$ and V_0. We have assumed $T_{ex}(2, 2) = T_{ex}(1, 1)$ and $\Delta V(2, 2) = \Delta V(1, 1)$ (for a discussion of these assumptions see Ho et al. 1979), and proceeded modelling the (2, 2) spectrum analogously to the (1, 1) case. The modelled spectra are shown in Figs. 1 and 2, together with the observed spectra and the residual spectra. The parameters determined in the χ^2-fits are given in Table 1.

The rotational temperature T_{12}, characterising the ratio of the populations in the $(J, K) = (2, 2)$ and $(J, K) = (1, 1)$ rotational states, can be calculated from

$$T_{12} = \frac{-41.5\ \mathrm{K}}{\ln\left(\frac{9}{20} \cdot \frac{\tau_0(2,2)}{\tau_0(1,1)}\right)} \qquad (1)$$

(combining Eqs. (2) and (3) of Ho et al. 1979). We find $T_{12} = 9.7 \pm 0.3$ K. The partition function is calculated assuming that only metastable $(J = K)$ rotational levels are populated and T_{12} is characteristic for all metastable levels and the ground state. The NH_3 column density calculated this

Table 1. Primary fitting parameters with formal errors as determined in the χ^2-fits shown in Figs. 1 and 2. We label τ_0 as the *total opacity* of the transition; it is the the sum of the central opacities of the individual hyperfine components (all Gaussian with $FWHM = \Delta V$) of the inversion transition in question. The small discrepancy between the two transitions in the line-of-sight velocities is also present in the (otherwise unused) second polarization channel. Possible reasons are a mispositioning of the spectrometers (by 0.2 channels), an inaccuracy in the rest frequency difference (of 2.8 kHz or 0.01%) or a combination of rotation (of the globule) and different opacities.

	Spectrum	
	$(J, K) = (1, 1)$	$(J, K) = (2, 2)$
$T_{\rm ex}$ (K)	6.4 ± 0.8	—
$\tau_0(J, K)$	7.2 ± 0.4	0.22 ± 0.03
V_0 (km s^{-1})	3.375 ± 0.002	3.34 ± 0.02
ΔV (km s^{-1})	0.181 ± 0.003	—

way is $N(NH_3) = 5.4 \times 10^{14}$ cm^{-2}. According to Walmsley & Ungerechts (1983) and Danby et al. (1988), T_{12} can be converted to the kinetic temperature, T. At low temperature they are almost equal, and we get $T = 9.9$ K. This temperature corresponds to a thermal line-width of $\Delta V_{\rm therm} = 0.164$ km s^{-1} ($\Delta V_{\rm therm} \equiv \sqrt{8 \ln 2 (kT)/(17 m_{\rm H})}$, where k is the Boltzmann constant and $m_{\rm H}$ the atomic hydrogen mass). See Harju et al. (1993) for the equations used to calculate $N(NH_3)$ and T.

The formal error of the temperature reflects only the rms noise. The calibration error plays no role, because the two lines were measured simultaneously and only their intensity *ratio* enters the temperature derivation. The true uncertainty of the kinetic temperature must be assessed through a critical review of the assumptions involved. As discussed by Ho et al. (1979), the most serious errors are probably the assumptions $T_{\rm ex}(1, 1) = T_{\rm ex}(2, 2)$ and $\eta(1, 1) = \eta(2, 2)$. As peculiar excitation conditions are unlikely to prevail in B68 (no internal heating sources and no large temperature gradients expected), we expect these differences to be $\lesssim$20%. Thus we have repeated our calculations assuming ±20% differences between the excitation temperatures and between the beam filling factors of the two transitions. The temperature uncertainty introduced by these differences turns out to be +12/−9%. Including the formal error from the fit, we finally derive $T = 9.9^{+1.3}_{-1.0}$ K.

We also used the Monte Carlo radiative transfer program developed by Juvela (1997) in order to test our previous approximation of near-homogeneous excitation conditions along the line of sight and this way checking our derived temperature value. The level energies were calculated from the analytical fit of Poynter & Kakar (1975), the radiative rates were calculated according to formulae in Townes & Schawlow (1955) and the collisional coefficients were taken from Danby et al. (1988).

As the absolute density of the underlying cloud model scales with the cloud's distance, we have run the program with several values of D (between 50 and 300 pc), each time optimising the fractional abundance, the turbulent line-width and the kinetic temperature. The best fits were obtained for $T = 9.7$ K (independent of D). The lowest χ^2 value was found for $D = 170$ pc, but no accurate determination is possible as values between 80 and 250 pc are all consistent with our calibration uncertainty. We also tried non-isothermal cloud models (with unchanged density structure) by coupling the kinetic temperature to the dust temperature (Zucconi et al. 2001) in the inner region of the globule (defined by $n > n_{\rm crit}$, trying $n_{\rm crit} = 10^4$, $10^{4.5}$ and 10^5 cm^{-3}). These temperature distributions did *not* improve the fits.

4. Discussion

4.1. Consistency with other temperature values

In Paper I we concluded that most likely the kinetic temperature in B68 is around 8 K. This was based on the measured $C^{18}O(J = 1–0)$ excitation temperature of 8 K and our Monte Carlo modelling results. Allowing for the possibility of subthermal excitation in the less dense outer parts, where most of the CO emission comes from, the kinetic temperature derived here is in agreement with our earlier CO measurements. Avery et al. (1987) deduced from their CO and ^{13}CO observations an outward increasing kinetic temperature between 6 and 11 K. As they used a constant fractional CO abundance, the derived gradient must be regarded with caution. However, the given range there covers the temperature derived here. Temperatures derived from ammonia in other globules without internal heating sources often lie around 10 K (Lemme et al. 1996). Galli et al. (2002) calculated the gas temperature distributions in molecular cloud cores and predicted for B68 a temperature of about 10 K, increasing only slightly towards the cloud edge.

There are two other attempts to derive the kinetic temperature of B68 by means of dedicated NH_3 inversion line observations: Bourke et al. (1995) derived $T = 16$ K. using the same underlying assumptions as we have used. As discussed in Paper I, this derivation is likely to involve some unfortunate error either in the calibration process or in the calculation. Very recently, Lai et al. (2002) have presented an estimate of the ammonia rotational temperature, which corresponds to a kinetic temperature of $T = 11.2 \pm 0.9$ K, which is consistent with our value.

4.2. Turbulence

The thermal line-width $\Delta V_{\rm therm} = 0.164 \pm 0.010$ km s^{-1} is only marginally smaller than the actual line-width $\Delta V = 0.181 \pm 0.003$ km s^{-1}, which is an essential condition for the BES premise of hydrostatic equilibrium. The internal support provided by turbulence is

$$E_{\rm turb} = \frac{2.33}{17} \left(\frac{\Delta V^2}{\Delta V^2_{\rm therm}} - 1 \right) E_{\rm therm} \,, \qquad (2)$$

where $E_{\rm therm}$ is the thermal energy and $2.33 m_{\rm H}$ is the mean molecular weight we assume throughout this paper. From our measurements we derive $E_{\rm turb}/E_{\rm therm} = 3\%$. The small contribution of the macroscopic motion is well below the uncertainty of the thermal energy and therefore it can be neglected as a physical parameter of the BES model.

4.3. Fixing the BES model

As mentioned in Sect. 1, after determination of the kinetic temperature the BES model of B68 is fixed if only one of the parameters n_c, D or gas-to-dust ratio is known. Using Eqs. (2) and (11) of Paper I we get for $T = 10$ K

$$N_c = 1.79 \times 10^{22}\ \mathrm{cm}^{-2} \left(\frac{n_c}{10^5\ \mathrm{cm}^{-3}}\right)^{1/2}$$
$$N_c = 2.59 \times 10^{22}\ \mathrm{cm}^{-2} \left(\frac{D}{100\ \mathrm{pc}}\right)^{-1} \quad (3)$$

and

$$N_c = 3.05 \times 10^{22}\ \mathrm{cm}^{-2} \left(\frac{N(\mathrm{H_2})/E(H-K)}{1.23 \times 10^{22}\ \mathrm{cm}^{-2}\ \mathrm{mag}^{-1}}\right).$$

In the third equation (the only one which does not require the BES assumptions to hold) we have assumed $N/N(\mathrm{H_2}) = 6/5$, and the term in brackets corresponds to the standard gas-to-dust ratio (Bohlin et al. 1978; Cardelli et al. 1989).

The number density of molecular hydrogen can be estimated from NH_3 data by balancing collisional excitation against emission (Ho & Townes 1983). However, to derive a value close to the *central* density, a high spatial resolution is required, which cannot be achieved with single-dish observations. As B68 has no detectable foreground stars, its distance is only known as far as its association with the Ophiuchus complex holds. According to de Geus et al. (1989) this molecular cloud complex extends from $D = 80$ to 170 pc with a central value of 125 pc. The gas-to-dust ratio is expected to vary from cloud to cloud, but there are a number of measurements suggesting that the variation does not exceed a factor of 2 (Paper I).

The relation between the distance and the gas-to-dust ratio imposed on B68 by the BES model reads

$$D = 85\ \mathrm{pc} \left(\frac{N(\mathrm{H_2})/E(H-K)}{1.23 \times 10^{22}\ \mathrm{cm}^{-2}\ \mathrm{mag}^{-1}}\right)^{-1}. \quad (4)$$

The globule is thus located on the near side of the Ophiuchus complex unless B68 has a *smaller* than average gas-to-dust ratio. The latter would be unexpected given the common understanding of dust evolution in cold and dense environments (Kim & Martin 1996). However, our Monte Carlo simulations preferred a distance in the 100–200 pc range so this possibility should not be ruled out. For the standard gas-to-dust ratio the mass and the external pressure of the BES are $M = 0.9\ M_\odot\ (D/85\ \mathrm{pc})$ and $P_R = 2.3 \times 10^{-12}$ Pa $(D/85\ \mathrm{pc})^{-2}$ respectively.

4.4. Ammonia abundance

The beam averaged ammonia column density has been calculated in Sect. 3. In order to get the fractional abundance $\chi(NH_3) = N(NH_3)/N(H_2)$, we have convolved the BES column density profile with a 40″ (*FWHM*) Gaussian. Taking into account that the observed position is 19″ off the position of maximum extinction (as reported by Bergin et al. 2002), the column density towards the peak extinction position is $N(NH_3) = 7.7 \times 10^{14}\ \mathrm{cm}^{-2}$, and with Eqs. (3) and (4) we get $\chi(NH_3) = 3.0 \times 10^{-8}$ $(D/85\ \mathrm{pc})$. This value is almost equal to the median value of a sample of 22 ammonia clumps in Orion (Harju et al. 1993) and very close to the fractional abundance in B217SW, a Taurus dense core with similar temperature and size as B68 (Hotzel et al. 2001).

5. Conclusions

Our observations support the hypothesis that B68 is in a state of isothermal hydrostatic equilibrium. Its kinetic temperature is 10 ± 1.2 K and its turbulent support is negligible. The ammonia abundance is close to the values found in other dark cores, but from the BES scaling relations we conclude that either the distance or the gas-to-dust ratio of B68 is smaller than previously expected.

Acknowledgements. We thank Dr. Floris van der Tak for providing the NH_3 collisional coefficients in electronic form. This project was supported by the Academy of Finland, grant Nos. 173 727 and 17 4854.

References

Alves, J. F., Lada, C. J., & Lada, E. A. 2001, Nature, 409, 159
Avery, L. W., White, G. J., Williams, I. P., & Cronin, N. 1987, ApJ, 312, 848
Barnard, E. E. 1919, ApJ, 49, 1
Bergin, E. A., Alves, J., Huard, T., & Lada, C. J. 2002, ApJ, 570, L101
Bohlin, R. C., Savage, B. D., & Drake, J. F. 1978, ApJ, 224, 132
Bourke, T. L., Hyland, A. R., Robinson, G., James, S. D., & Wright, C. M. 1995, MNRAS, 276, 1067
Cardelli, J. A., Clayton, G. C., & Mathis, J. S. 1989, ApJ, 345, 245
Danby, G., Flower, D. R., Valiron, P., Schilke, P., & Walmsley, C. M. 1988, MNRAS, 235, 229
de Geus, E. J., de Zeeuw, P. T., & Lub, J. 1989, A&A, 216, 44
Di Francesco, J., Hogerheijde, M. R., Welch, W. J., & Bergin, E. A. 2002, AJ, in press
Galli, D., Walmsley, M., & Gonçalves, J. 2002, A&A, 394, 275
Harju, J., Walmsley, C. M., & Wouterloot, J. G. A. 1993, A&AS, 98, 51
Ho, P. T. P., Barrett, A. H., Myers, P. C., et al. 1979, ApJ, 234, 912
Ho, P. T. P., & Townes, C. H. 1983, ARA&A, 21, 239
Hotzel, S., Harju, J., Juvela, M., Mattila, K., & Haikala, L. K. 2002, A&A, 391, 275 (Paper I)
Hotzel, S., Harju, J., Lemke, D., Mattila, K., & Walmsley, C. M. 2001, A&A, 372, 302
Juvela, M. 1997, A&A, 322, 943
Kim, S., & Martin, P. G. 1996, ApJ, 462, 296
Kukolich, S. G. 1967, Phys. Rev., 156, 83
Lai, S., Velusamy, T., Kuiper, T. B. H., & Langer, W. D. 2002, Poster #48 at the Conf. SFCHEM 2002, August 21–23, Waterloo, Canada
Lemme, C., Wilson, T. L., Tieftrunk, A. R., & Henkel, C. 1996, A&A, 312, 585
Ott, M., Witzel, A., Quirrenbach, A., et al. 1994, A&A, 284, 331
Poynter, R. L., & Kakar, R. K. 1975, ApJS, 29, 87
Townes, C. H., & Schawlow, A. L. 1955, Microwave Spectroscopy (New York: McGraw-Hill)
Walmsley, C. M., & Ungerechts, H. 1983, A&A, 122, 164
Zucconi, A., Walmsley, C. M., & Galli, D. 2001, A&A, 376, 650